International Journal of Nanomedicine

Dovepress
open access to scientific and medical research

Open Access Full Text Article

ORIGINAL RESEARCH

Host Immune Response Triggered by Graphene Quantum-Dot-Mediated Photodynamic Therapy for Oral Squamous Cell Carcinoma

This article was published in the following Dove Press journal:
International Journal of Nanomedicine

Xiliu Zhang[1]
Hongyu Li[1,*]
Chen Yi[1,*]
Guosheng Chen[2]
Ye Li[1]
Ying Zhou[1]
Guanhui Chen[1]
Yiming Li[1]
Yi He[1]
Dongsheng Yu[1]

[1]Guanghua School of Stomatology, Hospital of Stomatology, Sun Yat-Sen University, Guangdong Provincial Key Laboratory of Stomatology, Guangzhou 510055, People's Republic of China; [2]MOE Key Laboratory of Bioinorganic and Synthetic Chemistry, School of Chemistry, Sun Yat-Sen University, Guangzhou 510275, People's Republic of China

*These authors contributed equally to this work

Introduction: With the innovation of photosensitizers, photodynamic therapy is now widely used in antitumor detection and treatment. Graphene quantum dots (GQDs) are proposed as a promising alternative photosensitizer due to their high biocompatibility, specific photoactivity, and strong tumor concentration. However, the changes in host immunity triggered by GQDs have only rarely been reported.

Methods: In this work, GQDs as photosensitizers were conjugated to polyethylene glycol (PEG) to enhance solubility and blood circulation. The phototoxicity of the resulting GQD-PEG nanomaterials was then detected in vitro and in vivo. The antitumor immunity triggered by GQD-PEG under irradiation was further evaluated in an oral squamous cell carcinoma animal model.

Results: The obtained GQD-PEG nanomaterials exhibited low cytotoxicity, good solution stability, and excellent endocytosis. Both in vitro and in vivo, all demonstrated strong ablation for oral squamous cell carcinoma under irradiation. Meanwhile, host-immunity-related $CD8^+$ T cells (cytotoxic T lymphocytes) and proinflammatory cytokines, including IFN-γ and TNF-α, were significantly increased after photo-activated antitumor activity.

Conclusion: These results highlight the dominant role of GQD-PEG in photodynamic therapy and could have significant implications for further combination therapy as a promising antitumor immune response strategy triggered by nanomaterials.

Keywords: graphene quantum dots, photodynamic therapy, host immunity, oral squamous cell carcinoma

Introduction

Cancer immunotherapy is emerging as a promising treatment, with gradually increasing mortality of cancers and decreasing morbidity of young patients.[1,2] It relies on intervening in the body's inherent immunological system and augmenting antitumor responses. Because of its specific noninvasiveness and fewer side-effects, immunotherapy has become a powerful clinical strategy for treating various tumor types. However, it is still characterized by high cost, drug resistance, and limited efficacy in particular patients or tumor types.[3,4] Therefore, there is great interest in the development of a combination treatment strategy to enhance immune response.[5]

Photodynamic therapy (PDT) is a novel option for tumor ablation compared with conventional antitumor approaches such as chemotherapy and radiotherapy. As a well-established and photoactivated method, direct cancer ablation is based on the abundant toxicity of reactive oxygen species (ROS). Furthermore, a "domino effect" immune response is triggered by tumor-associated antigens released by

Correspondence: Dongsheng Yu
Guanghua School of Stomatology, Hospital of Stomatology, Sun Yat-Sen University, Guangdong Provincial Key Laboratory of Stomatology, Guangzhou 510055, People's Republic of China
Email yudsh@mail.sysu.edu.cn

submit your manuscript | www.dovepress.com
DovePress
http://doi.org/10.2147/IJN.S276153

apoptosis or necrosis cells. Multiple immune mechanisms are activated in the tumor microenvironment, inducing acute inflammation and antigen-presenting cells (APC) infiltration, further leading to the activation of T cells and augmenting host antitumor immunity.[6,7] Several studies have concentrated on photodynamic immunotherapy combined with an immune checkpoint blockade for tumor therapy. Wang et al[8] demonstrated that the combination of a PD-L1 blockade and PDT therapy exhibited significantly enhanced efficacy for the inhibition of primary and distant tumor growth, compared with either treatment alone. Yu et al[9] synthesized GO (HPPH)-PEG-HK particles as photosensitizers and observed not only primary tumor ablation but also distant lung metastasis suppression by the stimulation of dendritic cells (DCs) and the infiltration of $CD8^+$ T lymphocytes. Recent studies found that nanoparticles could be designed for a tumor microenvironment and increasing tissue penetration. Compared with 100-nm nanoparticles, 10-nm quantum dots facilitated lower immunogenicity, which could be used to optimize therapeutic-loaded nanoparticles.[10,11]

Graphene quantum dots (GQDs), zero-dimension graphene-derived materials, have a wide range of applications in the field of biomedicine due to their excellent physical and chemical properties. Currently, GQDs are attracting more interest in phototherapy, bioimaging, and drug delivery, due to their unique and tunable photoluminescence, derived from quantum confinement and edge effects.[12] Upon specific light-activation, GQDs have been proven to produce singlet oxygen and other ROS, which is key to the phototoxicity for PDT.[13,14] In addition, self-targeting in tumor tissue and the tunable emission wavelength of GQDs are of benefit for imaging and theranostics,[15,16] and the high water solubility and functional groups also render GQDs to be suitable drug nanocarriers.[17] It is reasonable to suppose that GQD-mediated photo-immunotherapy may emerge as a new antitumor strategy. Nevertheless, limited efforts have been devoted to addressing this topic.

Hence, in the present work, a hybrid photosensitizer based on pristine GQDs connected with polyethylene glycol (PEG) was proposed for applying PDT and evaluating the systematic immune change post-PDT. The obtained GQD-PEG exhibited dramatic ROS-generation efficacy and excellent biocompatibility under 560-nm laser irradiation. Meanwhile, both in vitro and in vivo study verified that the GQD-PEG showed strong ablation for oral squamous cell carcinoma under irradiation, compared with the control groups. We further demonstrated that antitumor immune-related cytotoxic T lymphocytes (CTL) and proinflammatory cytokines, including IFN-γ and TNF-α, were significantly increased after phototherapy (Figure 1). These results indicated that GQD-mediated photo-immunotherapy may become a good candidate for antitumor therapy.

Experimental Protocol

Materials

GQDs (100 mg, red fluorescence) were purchased from XFNANO Materials Tech Co., Ltd (Nanjing, China). NH_2-PEG-NH_2 (Mw=4 kDa) was obtained from SINOPEG (Xiamen, China).

N-(3-Dimethylaminopropyl)-N′-ethylcarbodiimide hydrochloride (EDC; 98%) and N-Hydroxysuccinimide (NHS; 98%) were purchased from aladdin (Shanghai, China). Singlet oxygen sensor green (SOSG) was obtained from Molecular Probes (Eugene, OR, USA). Fluorochrome-labeled CD3, CD4, and CD8 monoclonal antibodies were purchased from eBioscience (San Diego, CA, USA). Enzyme-linked immunosorbent assays (ELISA) of TNF-α and IFN-γ antibodies were also obtained from eBioscience.

Cell Lines and Animal Model

The human oral squamous cell carcinoma cell lines SCC 25 and SCC 9 and the normal cell line, human oral keratinocyte (HOK), were purchased from the ATCC and used for in vitro experiments. The murine SCC cell line SCC VII were used for in vivo experiments, which was provided by Professor Yixiang Wang, School of Stomatology, Peking University. Wild-type C3H mice (6- to 8-week-old females; weight, 18–20 g) were purchased from Vital River Laboratory Animal Technology Co., Ltd. (Beijing, China). The animal model for OSCC was established by subcutaneous injection of SCC VII cells into the right armpit of each mouse at 3.0×10^6 cells/mouse. The animal use based on SCC VII cells has been reviewed and approved by the Institutional Animal Care and Use Committee (IACUC), Sun Yat-Sen University (Approval Number: 2,019,000,249).

Synthesis of GQD-PEG

In the typical process, sonicate solution was initially used for 30 minutes at 700 W to achieve the necessary GQD dispersion. A 100-mg quantity of EDC and a 21.5-mg quantity of NHS were added to 2 mg/mL GQD solution for 2 h for activation of the carboxylic groups presenting on the surfaces

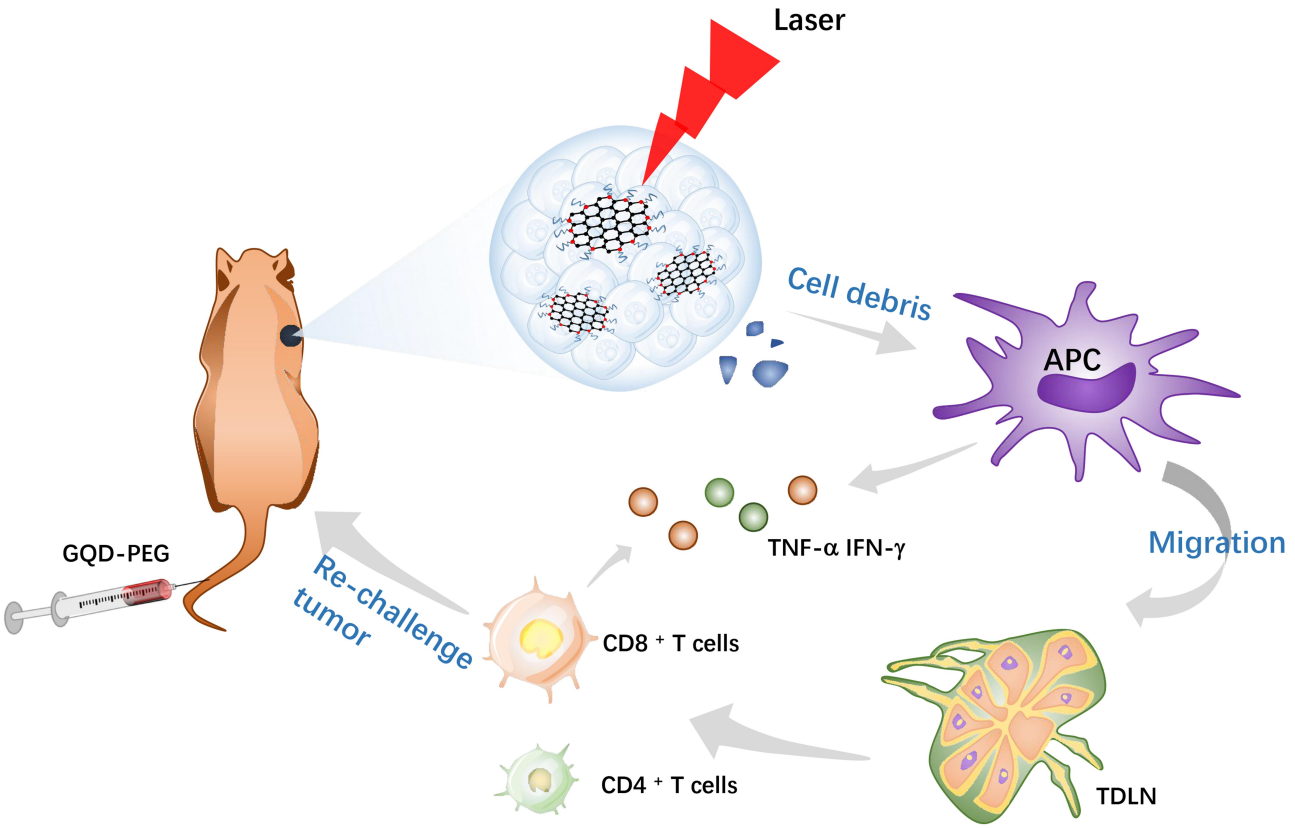

Figure 1 Schematic illustration of GQD-PEG-mediated photo-triggered immune responses for tumor therapy.

of GQDs. Then, a 250-mg quantity of NH_2-PEG-NH_2 was added to the solution and stirred overnight. For removal of the unattached PEG, the resulting mixture underwent dialysis for 72 h in 7 kDa dialysis membrane against water. Throughout, exposure to direct and strong light was avoided. The morphologies of GQD-PEG were visualized by transmission electron microscopy (TEM). Elemental composition and surface functional groups were analyzed by energy-dispersive spectroscopy (EDS) and Fourier transform infrared spectroscopy (FTIR). UV-vis absorption and fluorescence intensity were measured by UV-vis spectrophotometry.

Cellular Uptake

Cells were grown in DMEM/F12 (Gibco, Thermo Fisher Scientific, Inc., Waltham, MA, USA) supplemented with 10% fetal bovine serum (FBS; Gibco, Thermo Fisher Scientific, Inc.) at 37°C in a humidified atmosphere of 5% CO_2. For cell viability, cells were seeded in 96-well plates and cultured for 24 h, and then replaced with fresh medium containing series concentrations of GQD-PEG for another 12 h. A portion of viable cells was estimated with the Cell Counting Kit-8 assay (CCK-8). For observation of the cellular uptake of GQD-PEG, SCC 9 and human oral keratinocytes (HOK) were seeded in confocal Petri dishes (15 mm) at a density of 10^4 cells/mL and cultured for 24 h. Cells were then incubated with GQD-PEG or pristine GQD at a concentration of 50 μg/mL for 6 h and washed 3 times with phosphate-buffered saline (PBS; Hyclone, Logan, UT, USA). For the tracking of intracellular distribution, cells were stained with 4′,6-diamidino-2-phenylindole (DAPI) and observed by confocal laser scanning microscopy (CLSM; Zeiss, Jena, Germany). Fluorescence signals of nanomaterials were measured at a 560-nm excitation wavelength.

Singlet Oxygen Generation

The SOSG assay was utilized to detect the singlet production of $^1O_2$ by CLSM. For dose-dependent singlet oxygen generation, cells in 96-well plates were incubated with GQD-PEG for 50 μg/mL and then irradiated in 560 nm for 0, 1, 2, 3, 5, 10, and 15 minutes. The fluorescence signals of SOSG were detected by fluorimetric photometry at an excitation wavelength of 490 nm.

In vitro Photodynamic Therapy

For the assessment of antitumor activity of GQD-PEG, cells were seeded in 24-well plates at a density of

3.0×10^4 cells/mL and cultured with DMEM/F12. Twenty-four h later, cells were treated with GQD-PEG in a series of concentrations (25, 50, and 100 μg/mL) for 12 h and subjected to laser irradiation for 10 minutes. Following another 24-hour incubation, cell proliferation ability and cellular apoptosis were detected by the CCK-8 assay and flow cytometry, respectively. Cellular apoptosis was also visualized by means of a live/dead cell fluorescence staining assay (double-staining with calcein-AM and PI).

In vivo Imaging

The animal model for OSCC was established by subcutaneous injection of SCC VII cells into the right armpits of mice at 3.0×10^6 cells/mouse. SCC VII tumor-bearing C3H mice (n=3 per group) were intravenously injected with GQD-PEG at 200 μg per mouse. Tumor-bearing mice treated with PBS were utilized as controls. Four and 24 h post-injection, the mice were anesthetized by isoflurane, and their bodies were shaved. Fluorescence signals were detected by Xenogen IVIS Spectrum (Caliper Life Sciences, Hopkinton, MA, USA). The tumor uptake of GQD-PEG was measured by qualifying the fluorescence intensity of ROI with IVIS Spectrum software (Caliper Life Sciences, Hopkinton, MA, USA).

In vivo Phototoxicity and Immune Response

SCC VII tumor-bearing C3H mice were divided into 3 groups (n=5 per group), those treated with PBS, those treated with PBS and laser only, and those treated with GQD-PEG and laser. Mice were intravenously injected with 200 μg GQD-PEG and laser-irradiated (1 w/cm^2, 8 minutes) 4 h post-injection 3 times every 2 days. Tumor sizes were recorded every two days. Tumor volume was calculated in accordance with the equation: $V = W^2L/2$ (W, shortest diameter; L, longest diameter).

When tumors reached about 150 mm^3, the mice of all groups were sacrificed. Tumors were fixed with 4% paraformaldehyde for immunofluorescence detection. Tumor-draining lymph nodes from all 3 groups were isolated and digested to form a single-cell suspension. Cells were then stained with antibodies against CD3 (APC-Cyanine7), CD4 (FITC), and CD8 (PE), and then analyzed by flow cytometry. IFN-γ and TNF-α in the serum samples were collected and analyzed by ELISA kits. The body weights of C3H mice were measured every 2 days. At the end of the experimental process, the major organs of the mice in each group were harvested and sectioned into slices for histopathological evaluation, with H&E staining.

Statistical Analysis

All data are presented as means ± standard errors. Statistically significant differences were analyzed by one-way analysis of variance or Tukey's multiple-comparisons test when appropriate. $P < 0.05$ was considered a statistically significant difference. GraphPad Software 7.0 (GraphPad Software Inc., La Jolla, CA, USA), Origin pro 9.1 (OriginLab Corporation, Northampton, MA, USA), and GM 3.9 (Gatan DigitalMicrograph, Pleasanton, CA, USA) were used for statistical analyses. Every experiment was repeated at least 3 times.

Results and Discussion

Preparation and Characterization of GQD-PEG

The preparation process for GQD-PEG is illustrated in Figure 2A. Functionalization with PEG was shown to significantly improve the water solubility and enhance the biocompatibility of GQDs.[18,19] Herein, the appropriate molecular weight of NH_2-PEG-NH_2 (M_w=4000 Da) was chemically bonded with the carboxyl edges of GQDs. The obtained monodispersed GQD-PEG was observed under TEM imaging (Figure 2B). Particle size distribution measured by dynamic light-scattering indicated that the diameters of GQD-PEG were from 3 ~ 4 nm, in agreement with the results of TEM imaging (Figure 2C). The results obtained from the EDS spectrum were consistent with the expected elemental composition for GQD-PEG (Supporting Information, Figure S1), which confirmed the formation of N, C, and O as expected.[19] As shown in Figure 2D, the successful integration of PEG moieties with GQD was confirmed by FTIR. The absorption band at 1652 cm^{-1}, 1780 cm^{-1}, and 3426 cm^{-1} was assigned to the aromatic C=C, C=O, O–H stretching peak of GQD,[20] and the new characteristic band that emerged at 2887 cm^{-1} and 1113 cm^{-1} (C–H and C–O–C groups) was assigned to the integrated PEG moieties, respectively. As shown in Figure S2, GQD-PEG exhibited remarkable stability compared with pristine GQDs in all biological solutions (saline solution, PBS, serum, and DMEM), owing to the stabilizing effect of PEG. GQD-PEG inherited the UV absorption characteristics similar to those of GQDs (Figure S3), indicating the structural maintenance of GQDs after modification. In addition, the photoluminescence intensity of the GQDs (Figure 2E) in

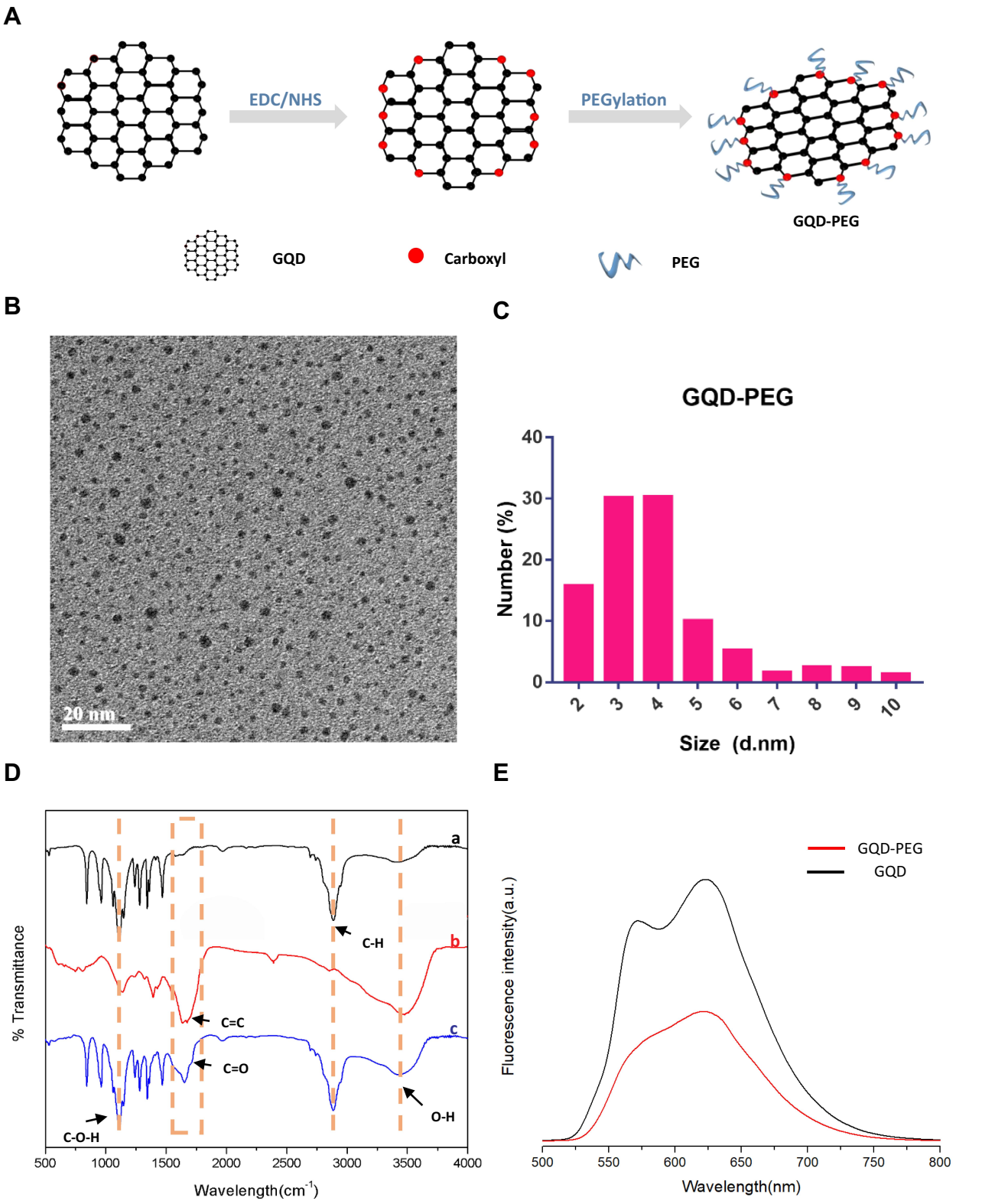

Figure 2 Characterization of GQD-PEG. (**A**) The preparation process of GQD-PEG. (**B**) TEM image of GQD-PEG. (**C**) Diameter distribution of GQD-PEG. (**D**) FTIR spectrum of (a) PEG, (b) GQD, and (c) GQD-PEG. (**E**) PL spectra of GQD-PEG at 560-nm excitation.

solution was decreased by PEG functionalization, which might result from the charge-transfer to the edges of GQDs after PEG functionalization.[18] Together, these results verified that the monodispersed GQD-PEG was successfully constructed.

In vitro Photodynamic Efficacy of GQD-PEG

GQDs are not only an alternative for photodynamic therapy, but also a promising carrier for immune drugs.[21,22] For evaluation of the therapeutic efficacy of GQD-PEG, the cytotoxicity of the resulting compound was evaluated in human SCC 9 and SCC 25 cells (Figures S4A, S4B). The cytotoxicity of GQD-PEG is dose-dependent, according to a CCK-8 assay reported previously.[23] After 12-hour incubation in the dark, the GQD-PEG group exhibited high cell viability for both SCC 9 and SCC 25 cells, even at high concentrations (100 μg/mL). Compared with the control group, cell viability of GQD-PEG groups was maintained at above 80% when the concentration was below 100 μg/mL. Therefore, we chose GQD-PEG concentrations below 100 μg/mL for the following in vitro study. Significant PDT efficacy of GQD-PEG was displayed upon laser irradiation (Figure 3A and B). After incubation with 100 μg/mL and light irradiation for 10 minutes, SCC 9 and SCC 25 cells showed variability decreases of 70% and 30%, respectively, in contrast to control groups. Meanwhile, a live/dead cell fluorescence staining assay further indicated that the photodynamic therapy group based on GQD-PEG was more effective in killing SCC 9 cells than were control groups with different concentrations, which was consistent with the CCK-8 assay (Figure 3C). As shown in Figure S5, analysis also demonstrated that early apoptosis and late apoptosis were increased to 5.31% and 5.12%, respectively, compared with the PBS group (0.10% and 0.05%) after treatment with 25 μg/mL concentration of GQD-PEG. These results all indicated the high phototoxicity of GQD-PEG in vitro.

Since specific targeting for tumor cells was essential for PDT efficacy, cellular internalization of GQD-PEG was investigated in SCC 9 and HOK. Figure 3D displays a panel of confocal fluorescent images of GQD-PEG and pristine GQD after 6 h of incubation. For tumor cell, both pristine GQD and GQD-PEG all exhibited similar strong accumulation in tumor cell nuclei and cytoplasm. Nonetheless, pristine GQD exhibited stronger accumulation in normal cell nuclei compared with GQD-PEG nanomaterials. This specific and differential accumulation may help further GQD-PEG applications in the field of phototherapy through the protection of normal tissue. As expected, SOSG detection further illustrated the strong phototoxicity of GQD-PEG under laser irradiation. GQD-PEG exhibited stronger $^1O_2$ production ability with increased irradiation (Figure 3E). Further, GQD-PEG exhibited significant potential as a light therapeutic agent for in vivo antitumor applications. In addition, GQD-PEG continued to exhibit high efficiency in PDT performance even with the interference of energy resonance transfer upon PEG functionalization.

In vivo Optical Imaging and Biodistribution Study

The carbon-dot-mediated nanoplatform has been shown to have the ability to increase the cellular uptake of nanoparticles and reduce unwanted side-effects.[24–26] Here, we report the first study of the biodistribution of GQD-PEG in SCC VII-bearing C3H mice, a classic animal model for OSCC.[27–29] From the in vivo imaging (Figure 4A), it can be seen that the main fluorescence signals of GQD-PEG groups are located primarily in the tumor tissue compared with those of the control groups. Four h after injection, the intensity of fluorescence signals in the tumor was the strongest, and a strong fluorescence signal was still observed up to 24 h. These findings may be because of the enhanced uptake ability and solution dispersion of GQD-PEG. The timely dissection of the main organs also demonstrated the existence of strong fluorescence in the tumor, whereas some fluorescence was observed in the liver and kidney (Figure 4B and C). These fluorescence signals detected in tumor and other tissues were probably due to the significant accumulation in the tumor and the slow metabolism of GQD-PEG. Specifically, GQD-PEG was able to accumulate efficiently in tumor areas and exhibit excellent pharmacokinetics, which was beneficial for PDT and drug delivery in vivo.[30]

In vivo Photoimmune Synergistic Antitumor Efficacy of GQD-PEG

Various studies have reported that non-invasive PDT was capable of inducing an effective response in a portion of OSCC without the risk of any serious side-effects.[31–33] These advantages might help establish PDT as the routine treatment for some OSCC, along with radiotherapy and chemotherapy. However, the widespread use of PDT requires more efficient phototoxicity and the potential of combination therapy. Encouraged by the antitumor effects

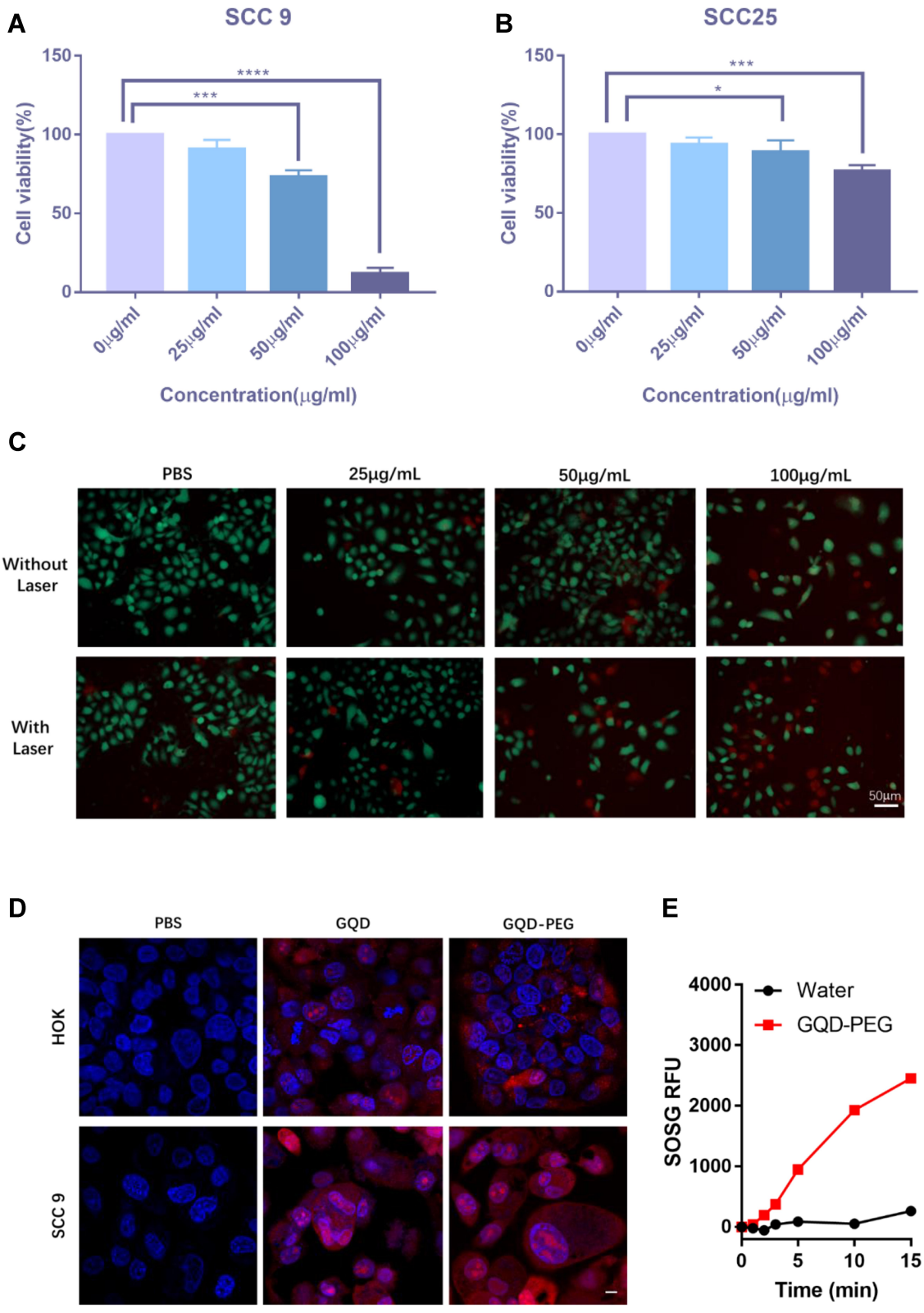

Figure 3 In vitro cytotoxicity of GQD-PEG. Cell viability of SCC 9 cells (**A**) and SCC 25 cells (**B**) incubated with GQD-PEG at different concentrations under irradiation. (**C**) Detection of cell viability using fluorescence probe (dead cells: red fluorescence of PI; live cells: green fluorescence of calcein). (**D**) Representative CLSM micrographs treated with pristine GQD and GQD-PEG for 6 h. Scale bar: 10 μm. (**E**) Singlet oxygen generation of GQD-PEG upon irradiation (560 nm, 1 W/cm^2). *P<0.05; ***P<0.001; ****P<0.0001.

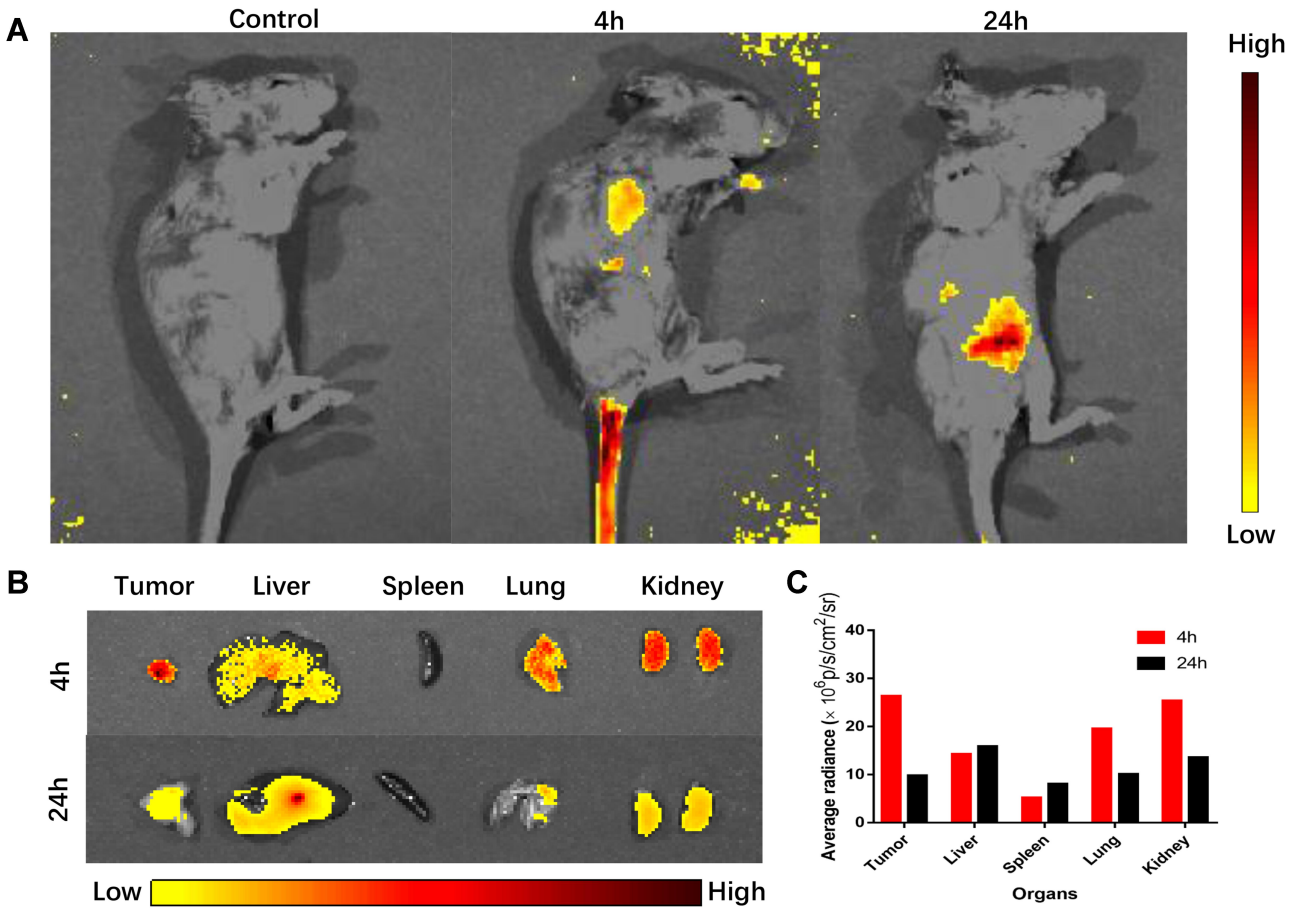

Figure 4 In vivo fluorescence imaging of GQD-PEG. (**A**) In vivo biodistribution of C3H mice after intravenous injection with GQD-PEG for 24 h, 4 h and 24 h post injection. (**B**) Ex vivo fluorescence imaging of major organs and (**C**) mean fluorescence intensity of the excised organs.

of PDT based on GQD-PEG in vitro and its remarkable tumor-targeting properties in vivo, we further investigated the antitumor efficiency of GQD-PEG with irradiation in SCC VII tumor-bearing C3H mice. Three groups, including PBS, PBS + laser, and GQD-PEG + laser, were evaluated once every other day on three consecutive occasions (Figure 5A). The tumor sizes and body weights of C3H mice were measured continuously during this process. Figure 5B displays the curves of tumor growth. The GQD-PEG group showed significantly inhibited tumor growth compared with the control and laser groups. The "GQD-PEG plus irradiation" group elicited tumor size reduction exceeding 70%, compared with those of the "laser only" and "PBS plus laser" groups. The direct antitumor efficacy might be attributable to the efficient tumor accumulations mediated by the enhanced permeability and retention (EPR) effect and the high $^1O_2$ toxicity induced from photoactivity. The average tumor weights were measured as 0.75 g, 0.45 g, and 0.11 g for groups treated with PBS, laser, and GQD-PEG plus irradiation, respectively (Figure 5C). The tumor images showed the excellent therapeutic efficacy of GQD-PEG with irradiation (Figure 5D). Figure 5E shows the changes of body weight of all treated mice. Because of the appropriate doses and intensities of treatments utilized, the weights of the mice showed slight increases with the different treatments.

Immune therapy as an emerging treatment was seen as an excellent combination therapy for PDT antitumor treatment because it is non-invasive and repeatable. Various nanoparticles have been demonstrated in specific photo-triggered tumor immunotherapy, as has their "domino effect" in the tumor microenvironment.[34–36] Without irradiation, GQDs have been proven to suppress proinflammatory T cell responses by potentiating the tolerogenic DC functions via the induction of autophagy.[37] A recent study also demonstrated that GQDs could alleviate immune-mediated central nervous system damage by modulating immune responses.[38] However, there has been no research focused on the GQD-PEG-mediated systematic immune response with irradiation. Here, the immunostimulatory activity of GQD-PEG was detected by

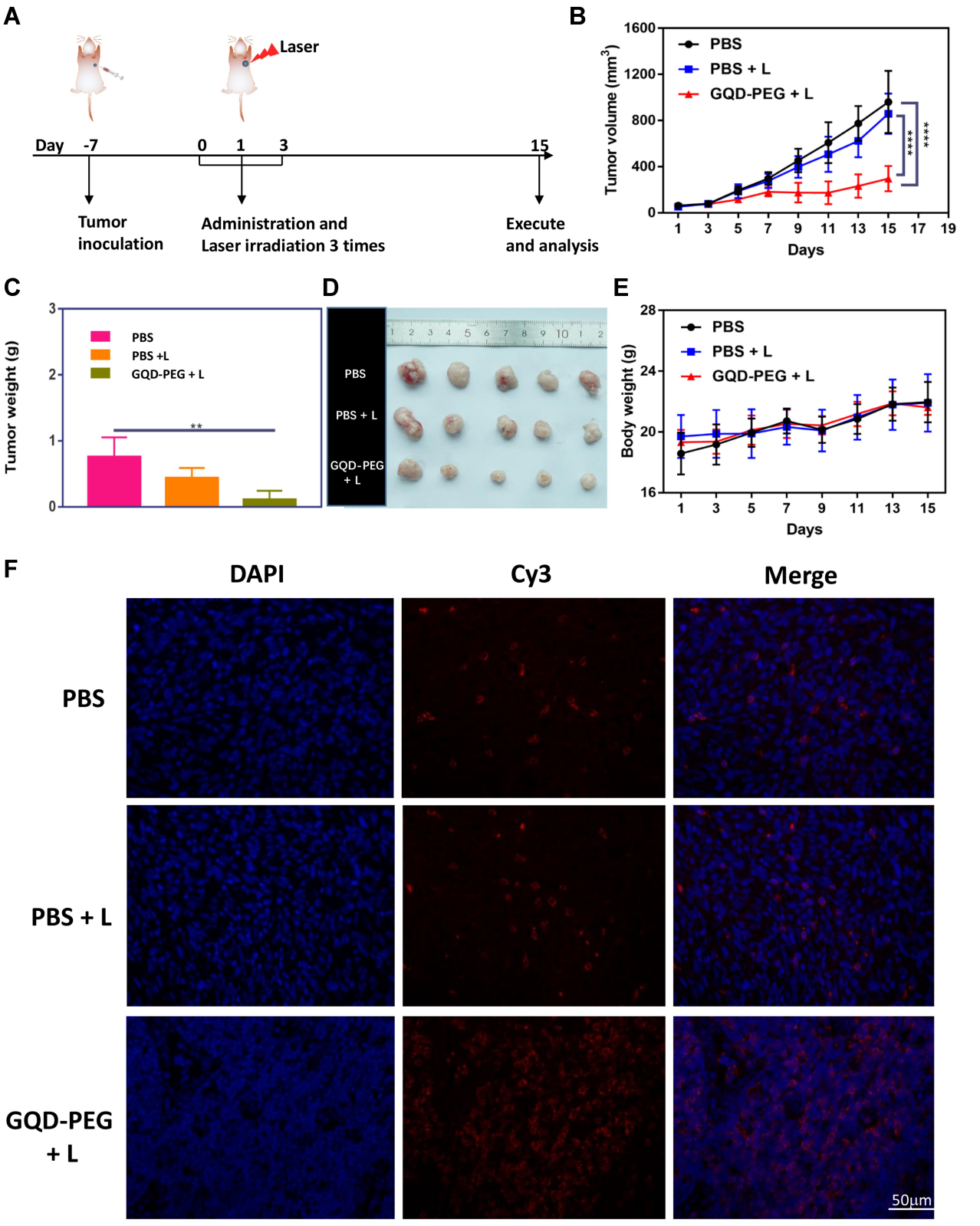

Figure 5 GQD-PEG-mediated photo-immune therapy. (**A**) Schematic overview of GQD-PEG-mediated photo-immune experimental workflow. (**B**) Tumor volume and (**D**) body weight curves of C3H mice from the different groups; (**C**) weight and (**E**) images of SCC VII tumors at the end of the experiment; (**F**) immunofluorescence staining of CD8a in the tumor tissues from mice after different treatments. ***P*<0.01; *****P*<0.0001.

flow cytometry and the ELISA assay. The levels of the representative proinflammatory cytokines, including TNF-α and IFN-γ, were detected in serum by ELISA. The laser groups could stimulate the secretion of TNF-α and IFN-γ compared with the control groups (Figure S6A). However, cytokine expression was significantly higher when treated with GQD-PEG under laser irradiation, which suggested that GQD-PEG could induce strong immune responses as a potential stimulator.[11,39] Previous studies have demonstrated that $CD4^+$T helper cells could activate cytotoxic cells such as cytotoxic T cells and natural killer cells. Meanwhile, mature DCs present the antigen peptide complex to $CD8^+$ cytotoxic T cells to form an MHC I–peptide complex, releasing cytotoxins (IFN-γ, perforin, granzymes, and granulysin) to kill cancer cells.[34,40] To examine whether GQD-PEG-mediated photoimmunotherapy could induce systemic immune responses, we evaluated the percentages of $CD3^+CD4^+$ T cells and $CD3^+$ $CD8^+$ T cells in tumor tissue at the end of the experiment. Flow cytometry results (Figure S6B) showed significantly increased percentages of $CD3^+$ $CD8^+$ T cells in the draining lymph tissues of the tumor. An immunofluorescence assay (Figure 5F) further confirmed the ability of GQD-PEG with laser to promote $CD8^+$ T cell infiltration into tumors. These results confirmed that the tumor areas of C3H mice treated with GQD-PEG under irradiation prompted $CD8^+$ cytotoxic T cell infiltration into the tumor tissue, enhancing the efficacy of its inhibition of tumor growth. Further, GQD-PEG did not cause any damage to the liver, lung, spleen, and kidney, which indicated its high biosafety to normal tissues (Figure S7). Above all, moderate GQD-PEG-mediated photoimmunotherapy photo-killed the tumor and released tumor-associated antigens, efficiently activating $CD8^+$ cytotoxic T cells with the help of cytotoxin-releasing TNF-α and IFN-γ, and resulting in systematic antitumor immunity. Although phototherapy could kill the tumor cells only upon irradiation, the more actively recruited immune cells may compensate for them during the continuing treatment cycle.[41–43]

Conclusion

In this work, GQD-PEG was synthesized and exhibited excellent water stability, a strong capacity for photodynamic efficiency, and immunostimulatory activity. After irradiation, the high ROS from photodynamic toxicity killed tumor cells and triggered immune responses by releasing endogenous tumor antigens. Subsequently, inflammatory cytokine secretion (TNF-α and IFN-γ) induced the recruitment of cytotoxic T lymphocytes to tumors to strengthen therapeutic efficacy. Moreover, fluorescence imaging demonstrated the tumor-targeting accumulation of GQD-PEG in vitro and in vivo. This study illustrated that GQD-PEG is a promising candidate for the combination of photodynamic and immunotherapy.

Acknowledgment

This article was supported by the National Natural Science Foundation of China (No. 81873711).

Disclosure

The authors declare no competing financial interest and report no conflicts of interest for this work.

References

1. Siegel RL, Miller KD, Jemal A. Cancer statistics, 2020. *CA Cancer J Clin*. 2020;70(1):7–30. doi:10.3322/caac.21590
2. Zhang B, Du W, Gan K, Fang Q, Zhang X. Significance of the neutrophil-to-lymphocyte ratio in young patients with oral squamous cell carcinoma. *Cancer Manag Res*. 2019;11:7597–7603. doi:10.2147/CMAR.S211847
3. Nam J, Son S, Park KS, Zou WP, Shea LD, Moon JJ. Cancer nanomedicine for combination cancer immunotherapy. *Nat Rev Mater*. 2019;4(6):398–414. doi:10.1038/s41578-019-0108-1
4. Pauken KE, Dougan M, Rose NR, Lichtman AH, Sharpe AH. Adverse events following cancer immunotherapy: obstacles and opportunities. *Trends Immunol*. 2019;40(6):511–523. doi:10.1016/j.it.2019.04.002
5. Duan XP, Chan C, Lin WB. Nanoparticle-mediated immunogenic cell death enables and potentiates cancer immunotherapy. *Angew Chem-Int Edit*. 2019;58(3):670–680. doi:10.1002/anie.201804882
6. Garg AD, Nowis D, Golab J, Agostinis P. Photodynamic therapy: illuminating the road from cell death towards anti-tumour immunity. *Apoptosis*. 2010;15(9):1050–1071. doi:10.1007/s10495-010-0479-7
7. Maeding N, Verwanger T, Krammer B. Boosting tumor-specific immunity using PDT. *Cancers*. 2016;8(10):91. doi:10.3390/cancers8100091
8. Wang D, Wang T, Liu J, et al. Acid-activatable versatile micelleplexes for PD-L1 blockade-enhanced cancer photodynamic immunotherapy. *Nano Lett*. 2016;16(9):5503–5513. doi:10.1021/acs.nanolett.6b01994
9. Yu X, Gao D, Gao L, et al. Inhibiting metastasis and preventing tumor relapse by triggering host immunity with tumor-targeted photodynamic therapy using photosensitizer-loaded functional nanographenes. *ACS Nano*. 2017;11(10):10147–10158. doi:10.1021/acsnano.7b04736
10. Riley RS, June CH, Langer R, Mitchell MJ. Delivery technologies for cancer immunotherapy. *Nat Rev Drug Discov*. 2019;18(3):175–196. doi:10.1038/s41573-018-0006-z
11. Wu C, Guan X, Xu J, et al. Highly efficient cascading synergy of cancer photo-immunotherapy enabled by engineered graphene quantum dots/photosensitizer/CpG oligonucleotides hybrid nanotheranostics. *Biomaterials*. 2019;205:106–119. doi:10.1016/j.biomaterials.2019.03.020
12. Zhang X, Wei C, Li Y, Yu D. Shining luminescent graphene quantum dots: synthesis, physicochemical properties, and biomedical applications. *Trends Anal Chem*. 2019;116:109–121. doi:10.1016/j.trac.2019.03.011
13. Yu Y, Mei L, Shi Y, et al. Ag-conjugated graphene quantum dots with blue light-enhanced singlet oxygen generation for ternary-mode highly-efficient antimicrobial therapy. *J Mater Chem B*. 2020;8(7):1371–1382. doi:10.1039/c9tb02300c

14. Ge J, Lan M, Zhou B, et al. A graphene quantum dot photodynamic therapy agent with high singlet oxygen generation. *Nat Commun*. 2014;5:4596. doi:10.1038/ncomms5596
15. Xu A, He P, Ye C, et al. Polarizing graphene quantum dots toward long-acting intracellular reactive oxygen species evaluation and tumor detection. *ACS Appl Mater Interfaces*. 2020;12 (9):10781–10790. doi:10.1021/acsami.9b20434
16. Lesani P, Singh G, Viray CM, et al. Two-photon dual-emissive carbon dot-based probe: deep-tissue imaging and ultrasensitive sensing of intracellular ferric ions. *ACS Appl Mater Interfaces*. 2020;12 (16):18395–18406. doi:10.1021/acsami.0c05217
17. Wei Z, Yin X, Cai Y, et al. Antitumor effect of a Pt-loaded nanocomposite based on graphene quantum dots combats hypoxia-induced chemoresistance of oral squamous cell carcinoma. *Int J Nanomed*. 2018;13:1505–1524. doi:10.2147/IJN.S156984
18. Novak TG, Kim J, Song SH, et al. Fast P3HT exciton dissociation and absorption enhancement of organic solar cells by PEG-functionalized graphene quantum dots. *Small*. 2016;12 (8):994–999. doi:10.1002/smll.201503108
19. Mihalache I, Radoi A, Munteanu C, Kusko M, Kusko C. Charge storage and memory effect in graphene quantum dots-PEG(600) hybrid nanocomposite. *Org Electron*. 2014;15(1):216–225. doi:10.1016/j.orgel.2013.10.031
20. Li Y, Wu Z, Du D, Dong H, Shi D, Li Y. A graphene quantum dot (GQD) nanosystem with redox-triggered cleavable PEG shell facilitating selective activation of the photosensitiser for photodynamic therapy. *RSC Adv*. 2016;6(8):6516–6522. doi:10.1039/c5ra23622c
21. Cao Y, Dong H, Yang Z, et al. Aptamer-conjugated graphene quantum dots/porphyrin derivative theranostic agent for intracellular cancer-related microRNA detection and fluorescence-guided photothermal/photodynamic synergetic therapy. *ACS Appl Mater Interfaces*. 2017;9(1):159–166. doi:10.1021/acsami.6b13150
22. Li S, Zhou S, Li Y, et al. Exceptionally high payload of the IR780 iodide on folic acid-functionalized graphene quantum dots for targeted photothermal therapy. *ACS Appl Mater Interfaces*. 2017;9 (27):22332–22341. doi:10.1021/acsami.7b07267
23. Zhang X, Wei C, Li Y, et al. Dose-dependent cytotoxicity induced by pristine graphene oxide nanosheets for potential bone tissue regeneration. *J Biomed Mater Res A*. 2020;108(3):614–624. doi:10.1002/jbm.a.36841
24. Yaghini E, Turner H, Pilling A, Naasani I, MacRobert AJ. In vivo biodistribution and toxicology studies of cadmium-free indium-based quantum dot nanoparticles in a rat model. *Nanomedicine*. 2018;14 (8):2644–2655. doi:10.1016/j.nano.2018.07.009
25. Comparetti EJ, Pedrosa VA, Kaneno R. Carbon nanotube as a tool for fighting cancer. *Bioconjug Chem*. 2018;29(3):709–718. doi:10.1021/acs.bioconjchem.7b00563
26. Goreham RV, Schroeder KL, Holmes A, Bradley SJ, Nann T. Demonstration of the lack of cytotoxicity of unmodified and folic acid modified graphene oxide quantum dots, and their application to fluorescence lifetime imaging of HaCaT cells. *Mikrochim Acta*. 2018;185(2):128. doi:10.1007/s00604-018-2679-8
27. Wang Y, Bi Q, Dong L, et al. Quinacrine enhances cisplatin-induced cytotoxicity in four cancer cell lines. *Chemotherapy*. 2010;56 (2):127–134. doi:10.1159/000313525
28. Li L, Cao B, Liang X, et al. Microenvironmental oxygen pressure orchestrates an anti- and pro-tumoral gammadelta T cell equilibrium via tumor-derived exosomes. *Oncogene*. 2019;38(15):2830–2843. doi:10.1038/s41388-018-0627-z
29. Korbelik M, Banath J, Zhang W, et al. Interaction of acid ceramidase inhibitor LCL521 with tumor response to photodynamic therapy and photodynamic therapy-generated vaccine. *Int J Cancer*. 2016;139 (6):1372–1378. doi:10.1002/ijc.30171
30. Shi S, Zhang L, Zhu M, et al. Reactive oxygen species-responsive nanoparticles based on PEGlated prodrug for targeted treatment of oral tongue squamous cell carcinoma by combining photodynamic therapy and chemotherapy. *ACS Appl Mater Interfaces*. 2018;10 (35):29260–29272. doi:10.1021/acsami.8b08269
31. Gondivkar SM, Gadbail AR, Choudhary MG, Vedpathak PR, Likhitkar MS. Photodynamic treatment outcomes of potentially-malignant lesions and malignancies of the head and neck region: a systematic review. *J Investig Clin Dent*. 2018;9(1). doi:10.1111/jicd.12270
32. Prazmo EJ, Kwasny M, Lapinski M, Mielczarek A. Photodynamic therapy as a promising method used in the treatment of oral diseases. *Adv Clin Exp Med*. 2016;25(4):799–807. doi:10.17219/acem/32488
33. Ren S, Cheng X, Chen M, et al. Hypotoxic and rapidly metabolic PEG-PCL-C3-ICG nanoparticles for fluorescence-guided photothermal/photodynamic therapy against OSCC. *ACS Appl Mater Interfaces*. 2017;9(37):31509–31518. doi:10.1021/acsami.7b09522
34. Rajendrakumar SK, Uthaman S, Cho CS, Park IK. Nanoparticle-based phototriggered cancer immunotherapy and its domino effect in the tumor microenvironment. *Biomacromolecules*. 2018;19 (6):1869–1887. doi:10.1021/acs.biomac.8b00460
35. Hou X, Tao Y, Pang Y, Li X, Jiang G, Liu Y. Nanoparticle-based photothermal and photodynamic immunotherapy for tumor treatment. *Int J Cancer*. 2018;143(12):3050–3060. doi:10.1002/ijc.31717
36. Saleem J, Wang L, Chen C. Carbon-based nanomaterials for cancer therapy via targeting tumor microenvironment. *Adv Healthc Mater*. 2018;7(20):e1800525. doi:10.1002/adhm.201800525
37. Tomic S, Janjetovic K, Mihajlovic D, et al. Graphene quantum dots suppress proinflammatory T cell responses via autophagy-dependent induction of tolerogenic dendritic cells. *Biomaterials*. 2017;146:13–28. doi:10.1016/j.biomaterials.2017.08.040
38. Tosic J, Stanojevic Z, Vidicevic S, et al. Graphene quantum dots inhibit T cell-mediated neuroinflammation in rats. *Neuropharmacology*. 2019;146:95–108. doi:10.1016/j.neuropharm.2018.11.030
39. Duan X, Chan C, Guo N, Han W, Weichselbaum RR, Lin W. Photodynamic therapy mediated by nontoxic core-shell nanoparticles synergizes with immune checkpoint blockade to elicit antitumor immunity and antimetastatic effect on breast cancer. *J Am Chem Soc*. 2016;138(51):6686–16695. doi:10.1021/jacs.6b09538
40. Dong H, Su H, Chen L, et al. Immunocompetence and mechanism of the DRibble-DCs vaccine for oral squamous cell carcinoma. *Cancer Manag Res*. 2018;10:493–501. doi:10.2147/CMAR.S155914
41. Song W, Kuang J, Li C-X, et al. Enhanced immunotherapy based on photodynamic therapy for both primary and lung metastasis tumor eradication. *ACS Nano*. 2018;12(2):1978–1989. doi:10.1021/acsnano.7b09112
42. Li L, Yang S, Song L, et al. An endogenous vaccine based on fluorophores and multivalent immunoadjuvants regulates tumor micro-environment for synergistic photothermal and immunotherapy. *Theranostics*. 2018;8(3):860–873. doi:10.7150/thno.19826
43. Nam J, Son S, Ochyl LJ, Kuai R, Schwendeman A, Moon JJ. Chemo-photothermal therapy combination elicits anti-tumor immunity against advanced metastatic cancer. *Nat Commun*. 2018;9(1):1074. doi:10.1038/s41467-018-03473-9